

W PAIRS PRODUCTION: SUBLEADING PROCESSES

Marta Łuszczak
in collaboration with Antoni Szczurek

Institute of Physics

University of Rzeszow

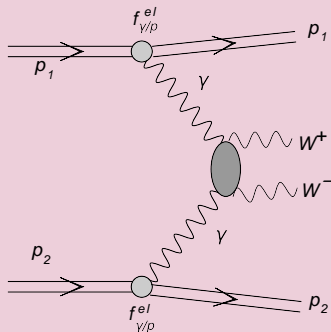
September 2-6, 2013
Heidelberg

Plan of the talk

- Introduction
- $\gamma\gamma \rightarrow W^+W^-$ reaction
- Inclusive production of W^+W^- pairs
 - $q\bar{q} \rightarrow W^+W^-$ mechanism
 - MRST-QED parton distributions
 - Naive approach to photon flux
 - Resolved photons
 - Single diffractive production
 - Results
- Conclusions

$pp \rightarrow ppW^+W^-$ reaction

The general diagram for the $pp \rightarrow ppW^+W^-$ reaction via $\gamma_{el}\gamma_{el} \rightarrow W^+W^-$ subprocess



$\gamma\gamma \rightarrow W^+W^-$ reaction

The three-boson $WW\gamma$ and four-boson $WW\gamma\gamma$ couplings, which contribute to the $\gamma\gamma \rightarrow W^+W^-$ process in the leading order:

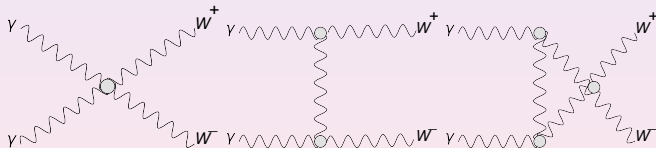
$$\begin{aligned}\mathcal{L}_{WW\gamma} &= -ie(A_\mu W_\nu^- \overleftrightarrow{\partial}^\mu W^{+\nu} + W_\mu^- W_\nu^+ \overleftrightarrow{\partial}^\mu A^\nu + W_\mu^+ A_\nu \overleftrightarrow{\partial}^\mu W^{-\nu}), \\ \mathcal{L}_{WW\gamma\gamma} &= -e^2(W_\mu^- W^{+\mu} A_\nu A^\nu - W_\mu^- A^\mu W_\nu^+ A^\nu),\end{aligned}$$

where the asymmetric derivative has the form

$$X \overleftrightarrow{\partial}^\mu Y = X \partial^\mu Y - Y \partial^\mu X.$$

$\gamma\gamma \rightarrow W^+W^-$ reaction

- The Born diagrams for the $\gamma\gamma \rightarrow W^+W^-$ subprocess

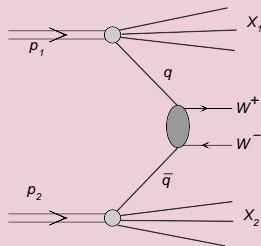


$\gamma\gamma \rightarrow W^+W^-$ reaction

The elementary tree-level cross section for the $\gamma\gamma \rightarrow W^+W^-$ subprocess can be written in the compact form in terms of the Mandelstam variables

$$\frac{d\hat{\sigma}}{d\Omega} = \frac{3\alpha^2\beta}{2\hat{s}} \left(1 - \frac{2\hat{s}(2\hat{s} + 3m_W^2)}{3(m_W^2 - \hat{t})(m_W^2 - \hat{u})} + \frac{2\hat{s}^2(\hat{s}^2 + 3m_W^4)}{3(m_W^2 - \hat{t})^2(m_W^2 - \hat{u})^2} \right),$$

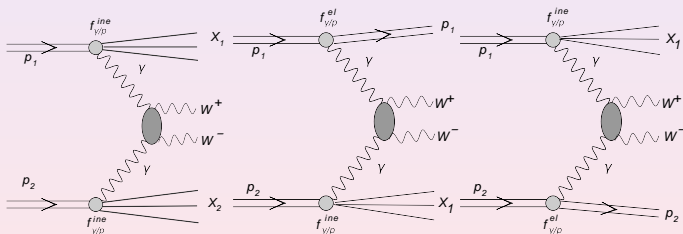
$\beta = \sqrt{1 - 4m_W^2/\hat{s}}$ is the velocity of the W bosons in their center-of-mass frame and the electromagnetic fine-structure constant $\alpha = e^2/(4\pi) \simeq 1/137$ for the on-shell photon

$q\bar{q} \rightarrow W^+W^-$ mechanism

The exclusive diffractive mechanism of central exclusive production of W^+W^- pairs in proton-proton collisions at the LHC (in which diagrams with intermediate virtual Higgs boson as well as quark box diagrams are included) was discussed in Ref. [P. Lebiedowicz, R. Pasechnik and A. Szczurek, Phys. Rev. **D81** \(2012\) 036003](#) and turned out to be negligibly small.

Inclusive $\gamma\gamma \rightarrow W^+W^-$ mechanism

If at least one photon is a “real” constituent of the nucleon then the mechanisms presented are possible:



MRSTQ parton distributions

The factorization of the QED-induced collinear divergences leads to QED-corrected evolution equations for the parton distributions of the proton.

$$\begin{aligned}\frac{\partial q_i(x, \mu^2)}{\partial \log \mu^2} &= \frac{\alpha_S}{2\pi} \int_x^1 \frac{dy}{y} \left\{ P_{qq}(y) q_i\left(\frac{x}{y}, \mu^2\right) + P_{qg}(y) g\left(\frac{x}{y}, \mu^2\right) \right\} \\ &+ \frac{\alpha}{2\pi} \int_x^1 \frac{dy}{y} \left\{ \tilde{P}_{qq}(y) e_i^2 q_i\left(\frac{x}{y}, \mu^2\right) + P_{q\gamma}(y) e_i^2 \gamma\left(\frac{x}{y}, \mu^2\right) \right\} \\ \frac{\partial g(x, \mu^2)}{\partial \log \mu^2} &= \frac{\alpha_S}{2\pi} \int_x^1 \frac{dy}{y} \left\{ P_{gq}(y) \sum_j q_j\left(\frac{x}{y}, \mu^2\right) + P_{gg}(y) g\left(\frac{x}{y}, \mu^2\right) \right\} \\ \frac{\partial \gamma(x, \mu^2)}{\partial \log \mu^2} &= \frac{\alpha}{2\pi} \int_x^1 \frac{dy}{y} \left\{ P_{\gamma q}(y) \sum_j e_j^2 q_j\left(\frac{x}{y}, \mu^2\right) + P_{\gamma\gamma}(y) \gamma\left(\frac{x}{y}, \mu^2\right) \right\}\end{aligned}$$

MRSTQ parton distributions

In addition to usual P_{qq} , P_{gq} , P_{qg} , P_{gg} splitting functions new splitting functions appear.

$$\tilde{P}_{qq} = C_F^{-1} P_{qq},$$

$$P_{\gamma q} = C_F^{-1} P_{gq},$$

$$P_{q\gamma} = T_R^{-1} P_{qg},$$

$$P_{\gamma\gamma} = -\frac{2}{3} \sum_i e_i^2 \delta(1-y)$$

momentum is conserved:

$$\int_0^1 dx \times \left\{ \sum_i q_i(x, \mu^2) + g(x, \mu^2) + \gamma(x, \mu^2) \right\} = 1$$

Cross section for photon-photon processes

$$\frac{d\sigma^{\gamma_{in}\gamma_{in}}}{dy_1 dy_2 d^2p_t} = \frac{1}{16\pi^2 \hat{s}^2} x_1 \gamma_{in}(x_1, \mu^2) x_2 \gamma_{in}(x_2, \mu^2) \overline{|\mathcal{M}_{\gamma\gamma \rightarrow W^+W^-}|^2}$$

- include only cases when nucleons do not survive a collision and nucleon debris is produced instead

Cross section for photon-photon processes

$$\frac{d\sigma^{\gamma in \gamma el}}{dy_1 dy_2 d^2 p_t} = \frac{1}{16\pi^2 \hat{s}^2} x_1 \gamma_{in}(x_1, \mu^2) x_2 \gamma_{el}(x_2, \mu^2) \overline{|\mathcal{M}_{\gamma\gamma \rightarrow W^+ W^-}|^2}$$
$$\frac{d\sigma^{\gamma el \gamma in}}{dy_1 dy_2 d^2 p_t} = \frac{1}{16\pi^2 \hat{s}^2} x_1 \gamma_{el}(x_1, \mu^2) x_2 \gamma_{in}(x_2, \mu^2) \overline{|\mathcal{M}_{\gamma\gamma \rightarrow W^+ W^-}|^2}$$
$$\frac{d\sigma^{\gamma el \gamma el}}{dy_1 dy_2 d^2 p_t} = \frac{1}{16\pi^2 \hat{s}^2} x_1 \gamma_{el}(x_1, \mu^2) x_2 \gamma_{el}(x_2, \mu^2) \overline{|\mathcal{M}_{\gamma\gamma \rightarrow W^+ W^-}|^2}$$

The **elastic photon fluxes** are calculated using the **Drees-Zeppenfeld parametrization**, where a simple parametrization of nucleon electromagnetic form factors was used

Naive approach to photon flux

- the photon distribution in the proton is a convolution of the distribution of quarks in the proton and the distribution of photons in the quarks/antiquarks

$$f_{\gamma/p} = f_q \otimes f_{\gamma/q}$$

which can be written mathematically as

$$xf_{\gamma/p}(x) = \sum_q \int_x^1 dx_q f_q(x_q, \mu^2) e_q^2 \left(\frac{x}{x_q} \right) f_{\gamma/q} \left(\frac{x}{x_q}, Q_1^2, Q_2^2 \right)$$

Naive approach to photon flux

- the flux of photons in a quark/antiquark was parametrized as:

$$f_\gamma(z) = \frac{\alpha_{em}}{2\pi} \frac{1 + (1-z)^2}{2} \log\left(\frac{Q_1^2}{Q_2^2}\right).$$

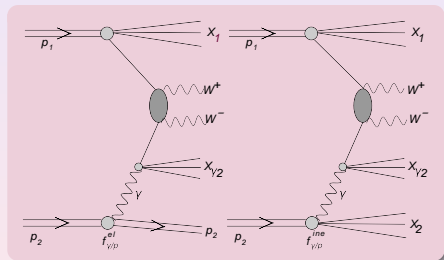
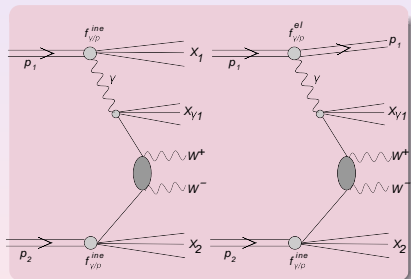
- the choice of scales:

$$Q_1^2 = \max(\hat{s}/4 - m_W^2, 1^2)$$

$$Q_2^2 = 1^2$$

$$\mu^2 = \hat{s}/4.$$

Resolved photons



Resolved photons

- extra photon remnant debris (called $X_{\gamma,1}$ or $X_{\gamma,2}$ in the figure) appears in addition
- the “photonic” quark/antiquark distributions in a proton must be calculated first as the convolution:

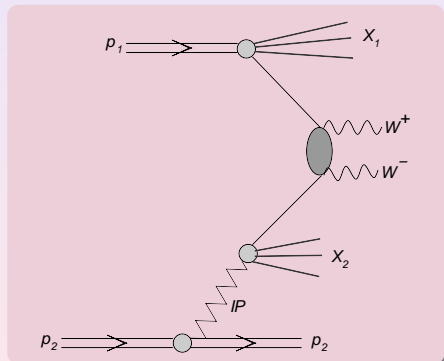
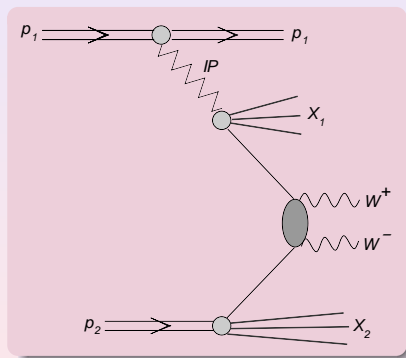
$$f_{q/p}^{\gamma} = f_{\gamma/p} \otimes f_{q/\gamma}$$

which mathematically means:

$$xf_{q/p}^{\gamma}(x) = \int_x^1 dx_{\gamma} f_{\gamma/p}(x_{\gamma}, \mu_s^2) \left(\frac{x}{x_{\gamma}} \right) f \left(\frac{x}{x_{\gamma}}, \mu_h^2 \right) .$$

Technically first $f_{\gamma/p}$ in the proton is prepared on a dense grid for $\mu_s^2 \sim 1 \text{ GeV}^2$ (virtuality of the photon) and then used in the convolution formula. The second scale is evidently hard $\mu_h^2 \sim M_{WW}^2$. The new quark/antiquark distributions of photonic origin are used to calculate cross section as for the standard quark-antiquark annihilation subprocess.

Single diffractive production of W^+W^- pairs



Single diffractive production of W^+W^- pairs

- apply the resolved pomeron approach
- one assumes that the Pomeron has a well defined partonic structure, and that the hard process takes place in a Pomeron–proton or proton–Pomeron (single diffraction) or Pomeron–Pomeron (central diffraction) processes.

$$\frac{d\sigma_{SD}}{dy_1 dy_2 dp_t^2} = K \frac{|M|^2}{16\pi^2 \hat{s}^2} \left[\left(x_1 q_f^D(x_1, \mu^2) x_2 \bar{q}_f(x_2, \mu^2) \right) \right. \\ \left. + \left(x_1 \bar{q}_f^D(x_1, \mu^2) x_2 q_f(x_2, \mu^2) \right) \right],$$
$$\frac{d\sigma_{CD}}{dy_1 dy_2 dp_t^2} = K \frac{|M|^2}{16\pi^2 \hat{s}^2} \left[\left(x_1 q_f^D(x_1, \mu^2) x_2 \bar{q}_f^D(x_2, \mu^2) \right) \right. \\ \left. + \left(x_1 \bar{q}_f^D(x_1, \mu^2) x_2 q_f^D(x_2, \mu^2) \right) \right]$$

The matrix element squared for the $q\bar{q} \rightarrow W^+W^-$ process is the same as previously for non-diffractive processes

Formalism

The 'diffractive' quark distribution of flavour f can be obtained by a convolution of the **flux of Pomerons** $f_{\mathbf{P}}(x_{\mathbf{P}})$ and the **parton distribution in the Pomeron** $q_{f/\mathbf{P}}(\beta, \mu^2)$:

$$q_f^D(x, \mu^2) = \int dx_{\mathbf{P}} d\beta \delta(x - x_{\mathbf{P}}\beta) q_{f/\mathbf{P}}(\beta, \mu^2) f_{\mathbf{P}}(x_{\mathbf{P}}) = \int_x^1 \frac{dx_{\mathbf{P}}}{x_{\mathbf{P}}} f_{\mathbf{P}}(x_{\mathbf{P}}) q_{f/\mathbf{P}}\left(\frac{x}{x_{\mathbf{P}}}, \mu^2\right).$$

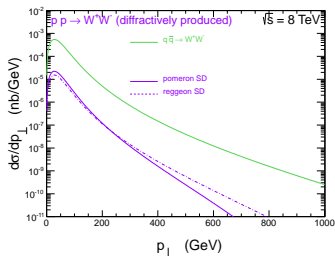
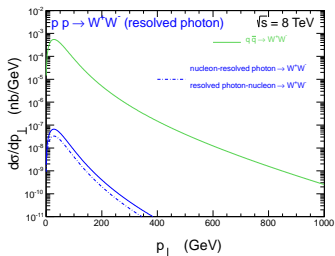
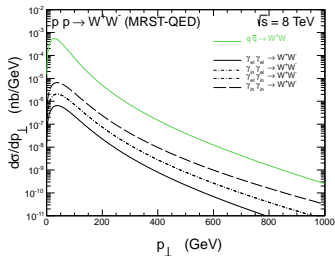
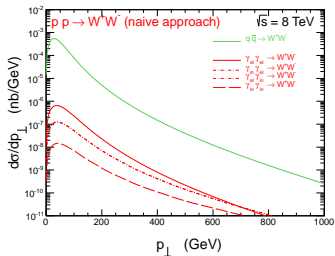
The flux of Pomerons $f_{\mathbf{P}}(x_{\mathbf{P}})$:

$$f_{\mathbf{P}}(x_{\mathbf{P}}) = \int_{t_{min}}^{t_{max}} dt f(x_{\mathbf{P}}, t),$$

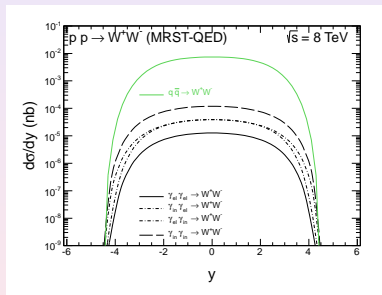
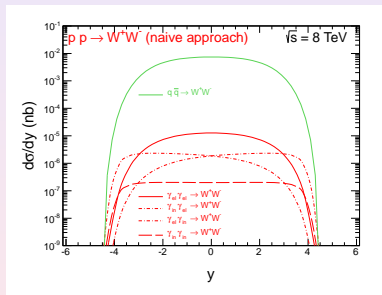
with t_{min} , t_{max} being kinematic boundaries.

Both pomeron flux factors $f_{\mathbf{P}}(x_{\mathbf{P}}, t)$ as well as quark/antiquark distributions in the pomeron were taken from the H1 collaboration analysis of diffractive structure function at HERA.

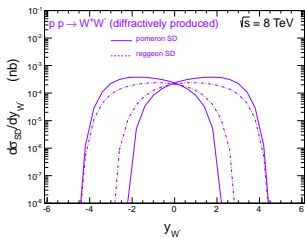
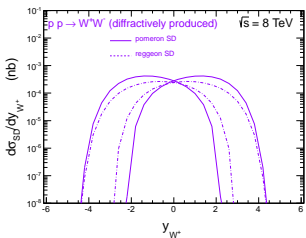
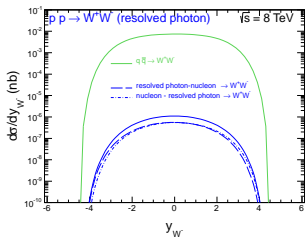
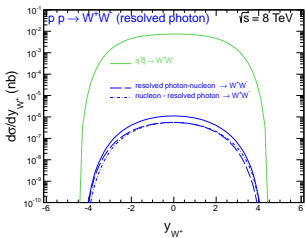
Results



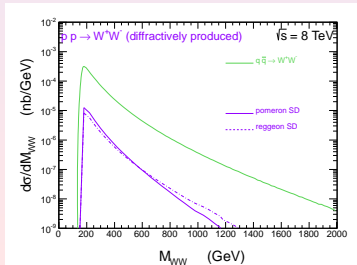
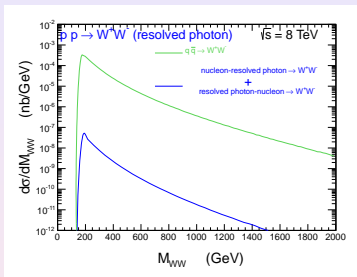
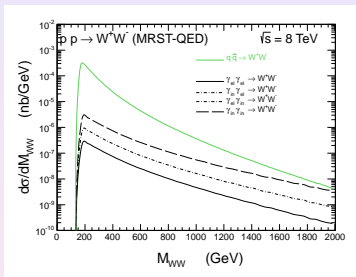
Results



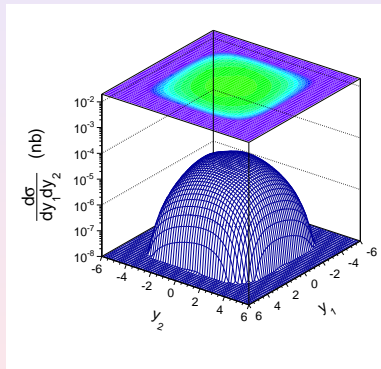
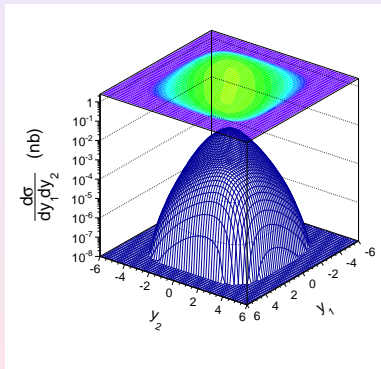
Results



Results



Results



Results

Contributions of different subleading processes to the total cross section (pb)

contribution	1.96 TeV	7 TeV	8 TeV	14 TeV	comment
CDF	12.1 pb				
D0	13.8 pb				
ATLAS		54.4 pb			large extrapolation
CMS		41.1 pb			large extrapolation
$q\bar{q}$	2.56	27.24	33.04	70.21	dominant (LO, NLO)
gg	$5.17 \cdot 10^{-2}$	1.48	1.97	5.87	subdominant (NLO)
$\gamma_{el}\gamma_{el}$	$3.07 \cdot 10^{-3}$	$4.41 \cdot 10^{-2}$	$5.40 \cdot 10^{-2}$	$1.16 \cdot 10^{-1}$	new, anomalous $\gamma\gamma WW$
$\gamma_{el}\gamma_{in}$	$1.08 \cdot 10^{-2}$	$1.40 \cdot 10^{-1}$	$1.71 \cdot 10^{-1}$	$3.71 \cdot 10^{-1}$	new, anomalous $\gamma\gamma WW$
$\gamma_{in}\gamma_{el}$	$1.08 \cdot 10^{-2}$	$1.40 \cdot 10^{-1}$	$1.71 \cdot 10^{-1}$	$3.71 \cdot 10^{-1}$	new, anomalous $\gamma\gamma WW$
$\gamma_{in}\gamma_{in}$	$3.72 \cdot 10^{-2}$	$4.46 \cdot 10^{-1}$	$5.47 \cdot 10^{-1}$	1.19	anomalous $\gamma\gamma WW$
$\gamma_{el, res} - q/\bar{q}$	$1.04 \cdot 10^{-4}$	$2.94 \cdot 10^{-3}$	$3.83 \cdot 10^{-3}$	$1.03 \cdot 10^{-2}$	new, quite sizeable
$q/\bar{q} - \gamma_{el, res}$	$1.04 \cdot 10^{-4}$	$2.94 \cdot 10^{-3}$	$3.83 \cdot 10^{-3}$	$1.03 \cdot 10^{-2}$	new, quite sizeable
$\gamma_{in, res} - q/\bar{q}$					new, quite sizeable
$q/\bar{q} - \gamma_{in, res}$					new, quite sizeable
double scattering(++)	$0.57 \cdot 10^{-2}$	0.11	0.14	0.40	not included in NLO studies
Pp	$2.82 \cdot 10^{-2}$	$9.88 \cdot 10^{-1}$	1.27	3.35	new, relatively small
pP	$2.82 \cdot 10^{-2}$	$9.88 \cdot 10^{-1}$	1.27	3.35	new, relatively small
Rp	$4.51 \cdot 10^{-2}$	$7.12 \cdot 10^{-1}$	$8.92 \cdot 10^{-1}$	2.22	new, relatively small
pR	$4.51 \cdot 10^{-2}$	$7.12 \cdot 10^{-1}$	$8.92 \cdot 10^{-1}$	2.22	new, relatively small

Conclusions

- Large contribution of photon induced processes
- Inelastic-inelastic photon-photon contribution large when photon treated as parton in the nucleon
- Resolved photon contribution are rather small
- In the future we have to include decays of W bosons